DOI: 10.1002/anie.201210294

Organic–Inorganic Hybrid Compounds

Layered Nanojunctions for Hydrogen-Evolution Catalysis**

Yidong Hou, Anders B. Laursen, Jinshui Zhang, Guigang Zhang, Yongsheng Zhu, Xinchen Wang, Søren Dahl, and Ib Chorkendorff**

The production of chemical fuels by using sunlight is an attractive and sustainable solution to the global energy and environmental problems. Photocatalytic water splitting is a promising route to capture, convert, and store solar energy in the simplest chemical compound (H_2).[1] Since the initial report of a photoelectrochemical cell using Pt-TiO_2 electrodes for hydrogen evolution by Fujishima and Honda in 1972, considerable studies have been focused on the development of highly efficient and stable photocatalyst powder systems, and especially on using earth-abundant semiconductors and co-factors for water splitting.[2] In practice, the achievement of the conversion of solar energy into hydrogen necessitates the spatial integration of semiconductors and co-catalysts to form surface junctions, so as to optimize the capture of light and to promote charge separation and surface catalytic kinetics.[3] The construction of effective surface junctions is therefore of vital importance, and not only strongly depends on the properties, such as crystal structure, band structure, and electron affinity, of both semiconductors and catalysts but also on the interface between the two materials.[4] In photocatalysis, an ohmic contact between photocatalysts and co-catalysts can allow the prompt migration of light-induced charge, thus resulting in an efficient photocatalytic reaction.

Recently, we found that graphitic carbon nitride (g-CN), a polymeric melon semiconductor with a layered structure analogous to graphite, meets the essential requirements as a sustainable solar energy transducer for water redox catalysis; these requirements include being abundant, highly-stable, and responsive to visible light.[5] g-CN is indeed a new type of visible-light photocatalyst that contains no metals, and has a suitable electronic structure ($E_g = 2.7$ eV, conduction band at -0.8 V and valence band at 1.9 V vs. RHE) covering the water-splitting potentials.[5] An improvement in the efficiency of H_2 production has been demonstrated by the introduction of nanohierarchical structures into g-CN.[6] It is noted that, like many other photocatalysts, g-CN alone shows very poor electrocatalytic activities for water splitting and relies on surface co-catalysts[7] to activate its photocatalytic functions. The co-catalyst cooperates with the light harvester to facilitate the charge separation and increases the lifetime of the photogenerated electron/hole pair, while lowering activation barriers for H_2 or O_2 evolution. Thus, the use of a co-catalyst leads to an increase in overall photocatalytic performance, including activity, selectivity, and stability. Generally, the efficiency of a given photocatalytic system is dependent on the ability of the co-catalysts to support reductive and/or oxidative catalysis. In particular, the structural characteristics and intrinsic catalytic properties of a co-catalyst are important. However, the study of the structural and electronic compatibility between g-CN and co-catalysts has been limited so far. The co-catalysts used are mainly platinum group metals or their oxides, which are scarce and expensive.[8] Photocatalytic/catalytic systems based on abundantly available materials are certainly desirable for large-scale hydrogen production for future energy production based on water and sunlight.

Among various hydrogen-evolution reaction (HER) catalysts, molybdenum sulfur complexes have received a lot of attention.[9] MoS_2 was found to be a good electrocatalyst for H_2 evolution, and the HER activity stemmed from the sulfur edges of the MoS_2 crystal layers.[10] When grown on graphene sheets, nanostructured MoS_2 exhibited excellent HER activity owing to the high exposure of the edges and the strong electronic coupling to the underlying planar support.[11] Incomplete cubane $[Mo_3S_4]^+$ clusters and amorphous MoS_2 are also proven HER catalysts.[12] Some of these HER catalysts have been used in photocatalytic H_2 production and they exhibited a remarkable promoting effect.[9,13]

MoS_2 has a similar structure to graphite; it has a layered crystal structure consisting of S–Mo–S "sandwiches" held together by van der Waals force. The fact that g-CN and MoS_2 have analogous layered structures should minimize the lattice mismatch and facilitate the planar growth of MoS_2 slabs over the g-CN surface,[15] thus constructing an organic–inorganic hybrid with graphene-like thin layered heterojunctions (Scheme 1 a). Such a distinct nanoscale structure has some advantages. It can increase the accessible area around the planar interface of the MoS_2 and g-CN layers and diminish the barriers for electron transport through the co-catalyst, thus facilitating fast electron transfer across the interface by the electron tunneling effect. Also, thin layers can lessen the light blocking effect of the co-catalyst, thus improving the light utilization by g-CN. Importantly, the intrinsic band structures

[*] Y. Hou, J. Zhang, G. Zhang, Y. Zhu, Prof. X. Wang
Research Institute of Photocatalysis, College of Chemistry and Chemical Engineering, Fuzhou University
Fuzhou 350002 (China)
E-mail: xcwang@fzu.edu.cn
A. B. Laursen, Prof. S. Dahl, Prof. I. Chorkendorff
Department of Physics, CINF, Technical University of Denmark
2800 Kongens Lyngby (Denmark)
E-mail: ibchork@fysik.dtu.dk

[**] Supported by the 973 Program (2013CB632405) and the National Natural Science Foundation of China (21203030, 21033003 and 21173043). This material is also based upon work funded by the Danish Ministry of Science for funding the Catalysis for Sustainable Energy (CASE) initiative and The Center for Individual Nanoparticle Functionality.

Supporting information for this article is available on the WWW under http://dx.doi.org/10.1002/anie.201210294.

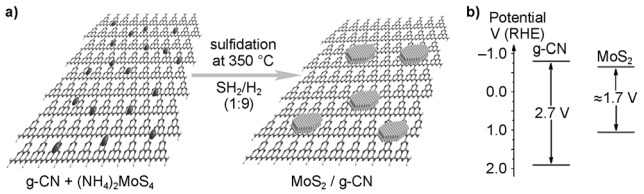

Scheme 1. a) The procedure for gas-phase sulfidation and the idealized structural model of the resultant MoS_2/g-CN layered junctions, b) Band energy diagrams for g-CN[5] and thin MoS_2.[14]

of g-CN and MoS_2 provide the possibility of the directional migration of photogenerated electrons from g-CN to MoS_2 (Scheme 1 b), while keeping sufficient chemical potential in the electrons to react with protons to produce hydrogen at HER active sites of MoS_2.[10] For all these reasons, MoS_2 is a promising candidate as a non-noble metal co-catalyst for g-CN photocatalyst, when the combination of its geometrical and electronic advantages is taken into consideration. Herein, we report the synthesis of earth-abundant organic–inorganic layered heterojunctions by gas-controlled growth of thin-layered MoS_2 on a mesoporous g-CN (mpg-CN) surface. These junctions exhibited enhanced photocatalytic hydrogen-evolution activity under visible-light irradiation, and their performance was comparable to that of Pt/mpg-CN under our reaction conditions.

MoS_2/mpg-CN samples were synthesized by impregnating mpg-CN with an aqueous solution of $(NH_4)_2MoS_4$, and subsequent sulfidation with H_2S gas at 350 °C. The TEM image of 0.5 wt % MoS_2/mpg-CN in Figure 1 a shows that the MoS_2 has a typical layered structure and grows along the surface of mpg-CN. Note that the junctions are only stable under the electron beam for a short period of time, and extended exposure inevitably causes damage to the junctions.

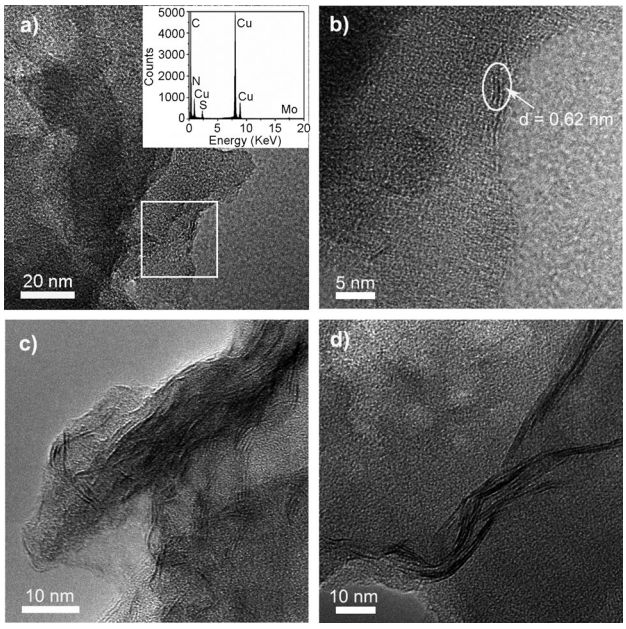

Figure 1. TEM images for MoS_2/g-CN. a–b) 0.5 wt % MoS_2/mpg-CN, the inset in (a) shows the energy-dispersive X-ray analysis of the sample; c) 0.5 wt % MoS_2/bulk g-CN; d) 0.5 wt % MoS_2 nanosheets/mpg-CN.

The nanoscale nature of MoS_2 and the polymeric nature of mpg-CN, together with their similar contrast under the TEM field also make the capture imaging of tight contacts difficult. Nevertheless, energy dispersive X-ray analysis performed on the area denoted by the rectangle in Figure 1 a confirmed the co-existence of Mo and S, with a molar ratio of S to Mo of approximately 2.5. The elements C and N together with Cu are also detected from the TEM grid.

The magnified HRTEM image in Figure 1 b displays a fringe with lattice spacing of approximately 0.62 nm, corresponding to the (002) plane of hexagonal MoS_2. The number of the MoS_2 slabs deposited on mpg-CN is approximately 1–3. For 0.5 wt % MoS_2/bulk g-CN, large and thick multiple layers of MoS_2 are observed on the g-CN surface (see Figure 1 c). MoS_2 and g-CN have analogous layered structures and the specific properties of the van der Waals force might provide an advantage in the junction formation. Intimate junctions between MoS_2 and g-CN are indeed formed by the sulfidation process. Note that the mesoporous structure facilitates and stabilizes the high dispersion of MoS_2 over the mpg-CN surface and the formation of the thin MoS_2/mpg-CN intimate junction. This thin junction ensures effective hydrogen evolution by virtue of the light absorption by mpg-CN combined with a short carrier transport distance, and the exposure of a large external surface area for the catalytic reaction. The thin layers of MoS_2 dispersed on the mpg-CN surface could also offer much higher efficiency than multi-layered MoS_2 owing to the electron-tunneling effect through the MoS_2 thin layers to reaction interfaces. We also loaded MoS_2 nanosheets onto mpg-CN by mixing an aqueous suspension of the exfoliated MoS_2 with mpg-CN. The long MoS_2 nanosheets aggregate together on the mpg-CN surface and ohmic loss occurs between mpg-CN and MoS_2 (Figure 1 d). Obviously, the aggregation and ohmic loss will be detrimental for fast charge transportation across the multi-layers to the solution as the probability of barrier penetration is exponentially dependent on the barrier thickness. A study of the photocatalytic hydrogen evolution should verify this hypothesis.

The chemical state of the MoS_2 that was loaded on the mpg-CN was carefully examined by X-ray photoemission spectroscopy (XPS). Strong Mo 3d5 and S 2s bands at 228.4 eV (Mo 3d A) and 225.9 eV (S 2s A), respectively, are present (Figure 2), thus indicating the dominant existence of Mo^{4+} and S^{2-}. This result is further confirmed by the S 2p core spectra (Figure S1). The binding energy of Mo is lower in value than has been previously reported,[10c] indicative of the strong chemical interaction (electron coupling) between the MoS_2 layers and the conjugated CN layers.[16] Small doublet sub-bands for Mo 3d at 233.1 (Mo 3d B) and 236.1 eV are also observed, suggesting the presence of Mo^{6+}, presumably owing to the formation of small amounts of surface oxide species.

The virtually identical X-ray diffraction patterns (Figure S2 in the Supporting Information) and FTIR spectra (Figure S3 in the Supporting Information) of mpg-CN and MoS_2/mpg-CN reveal that loading with MoS_2 does not change the bulk structure of mpg-CN and its core chemical skeleton. This finding means we can rule out a structural effect of mpg-CN in improving the hydrogen-production performance.

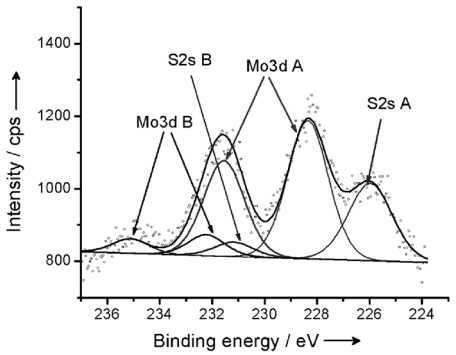

Figure 2. XPS spectra of 0.5 wt% MoS_2/mpg-CN.

Regarding the optical properties of MoS_2/mpg-CN, there is a broad absorption shoulder in the UV–Vis absorption spectra (see the Supporting Information, Figure S4). The absorption intensity increases with an increase in the amount of MoS_2, and corresponds to the optical absorption of MoS_2. Remarkably, the photoluminescence of mpg-CN (Figure 3a) is quenched in the presence of MoS_2. This occurrence is attributed to the efficient charge transfer between MoS_2 and mpg-CN, thus leading to an improvement in the separation efficiency of the light-stimulated carriers.

Electrochemical measurements were conducted in a typical three-electrode cell (see the Supporting Information for details). Cyclic voltammograms are shown in Figure 3b. The observed cathodic current in the range of −1.2–−1.5 V versus Ag/AgCl (−0.6–−0.9 V vs. RHE) can be ascribed to the H_2 evolution. Compared to pure mpg-CN, MoS_2/mpg-CN shows a much higher activity. This result indicates that MoS_2 can efficiently electrocatalyze the evolution of H_2, consequently, improving the HER performance of MoS_2/mpg-CN over mpg-CN. The charge transfer rate in the dark was studied by electrochemical impedance spectroscopy (EIS; Figure 3c)and the expected semicircular Nynquist plots for mpg-CN and MoS_2/mpg-CN, with a significantly decreased diameter for MoS_2/mpg-CN, were obtained. This result implies that MoS_2/mpg-CN indeed has improved hydrogen-evolution kinetics compared to the mpg-CN polymer.

Photocatalytic hydrogen-evolution experiments were carried out by using MoS_2/mpg-CN powder and lactic acid (as a sacrificial agent), with visible-light illumination. Table S1 (see the Supporting Information) shows the rate of H_2 evolution on the MoS_2/mpg-CN catalysts, together with other catalysts for comparison. No H_2 was detected when MoS_2 was supported on inert mesoporous SiO_2 (SBA-15), thus implying that MoS_2 alone is not active for photocatalytic H_2 evolution in a wireless system (see the Supporting Information, Table S1). mpg-CN alone also shows negligible activity, thus indicating that mpg-CN has poor hydrogen-evolution kinetics. Even when mixed with MoS_2 nanosheets, which are an effective HER catalyst,[17] mpg-CN still exhibits poor activity; this result indicates that the intimate contact between MoS_2 and mpg-CN is crucial for forming an effective charge–separation nanojunction. An in situ growth method involving impregnation and subsequent sulfidation is a successful way to prepare the active MoS_2/mpg-CN nanojunction. The thus obtained MoS_2/mpg-CN show high activities: the hydrogen-evolution rate over 0.5 wt% MoS_2/mpg-CN reaches 20.6 μmol h^{-1}, which is higher than that of 0.5 wt% Pt/mpg-CN (4.8 μmol H_2 h^{-1}, shown in Figure 4a).

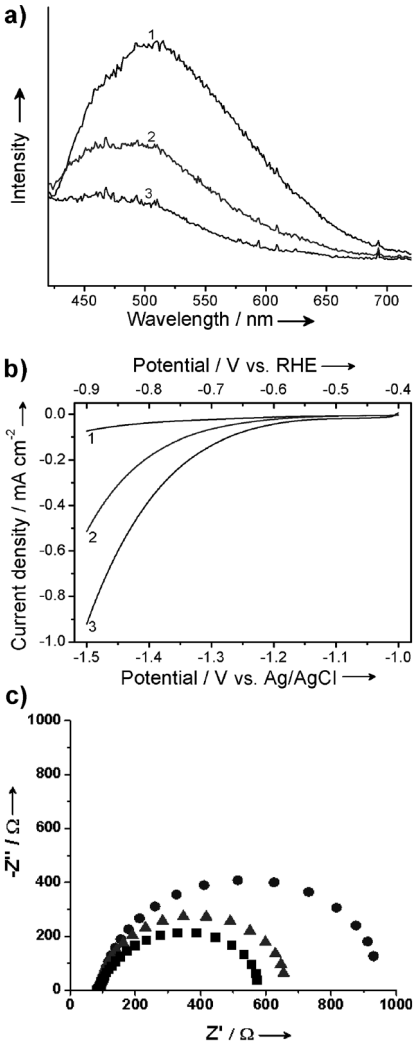

Figure 3. a) Photoluminescence spectra of mpg-CN (1) 0.5 wt% MoS_2/mpg-CN (2) and 2.0 wt% MoS_2/mpg-CN (3). b) Polarization curves of mpg-CN (1) 0.5 wt% MoS_2/mpg-CN (2) and 2.0 wt% MoS_2/mpg-CN (3) electrodes in 0.5 M Na_2SO_4 solution. c) Nyquist plots of electrochemical impedance spectroscopy with mpg-CN (●) 0.5 wt% MoS_2/mpg-CN (▲) and 2.0 wt% MoS_2/mpg-CN (■) electrodes at −1.5 V vs. Ag/AgCl (−0.9 V vs. RHE).

A plot of the variation in activity of mpg-CN loaded with different amounts of MoS_2 (Figure 4a) shows that the rate of hydrogen evolution increases initially, and then reaches a maximum when the amount of MoS_2 loaded is about 0.2 wt%. A further increase in the amount of MoS_2 results in a decrease in the photocatalytic hydrogen evolution. The decrease in the activity of samples with a heavy loading of MoS_2 is likely due to the shading effect, which can seriously block the absorption of the incident light by mpg-CN. This hypothesis is supported by the UV–Vis spectra. Additionally, because of the anisotropic conductivity of MoS_2,[18] thin-layered MoS_2 can lessen the poor charge transport from layer

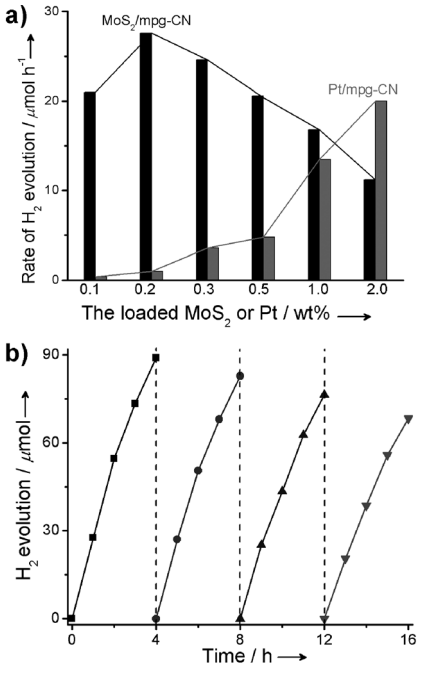

Figure 4. a) The rate of H_2 production over mpg-CN loaded with different amounts of MoS_2 or Pt, b) Cycle runs for the photocatalytic H_2 production over 0.2 wt% MoS_2/mpg-CN.

to layer and shorten the electron transport time and distance, thus improving the efficiency in the utilization of photogenerated electrons for hydrogen production. These explain the best activity of 0.2 wt% MoS_2/mpg-CN, with an apparent quantum yield of 2.1% measured at 420 nm.

Prolonged irradiation with visible light of 16 h ($\lambda >$ 420 nm) was also performed. The total amount of H_2 produced (ca. 310 μmol) far exceeded the molar amounts of both MoS_2 (ca. 0.25 μmol) and the photocatalyst (ca. 108 μmol). On the basis of the amount of loaded MoS_2, the turnover number (TON) was about 1240. There is no doubt that the reaction indeed proceeds catalytically.

The activity test demonstrated that the catalyst became deactivated when recycled (Figure 4b). To reveal the reason for this deactivation, we did a comparison of the X-ray photoelectron spectra of the fresh and used MoS_2/mpg-CN. The XPS analysis (Figure S1) shows that N 1s and C 1s core level spectra are the same for the fresh and used photocatalysts, thus implying the high stability of mpg-CN. However, changes are observed in the Mo 3d and S 2s core level spectra. The data obtained after deconvolution of these peaks (see the Supporting Information, Table S2) reveals that the atomic ratios of Mo^{6+}/N and S^{6+}/N increase and S^{2-}/N decreases. This finding means that the oxidation/corrosion of MoS_2 by photogenerated holes occurs over the MoS_2/mpg-CN catalysts, accounting for its deactivation during the prolonged operations. Further studies on photocatalysts based on organic–inorganic hybrid layered heterojunctions is still needed to improve the activity and stability for practical applications.

Particularly, the surface kinetic controls to inhibit MoS_2 corrosion by adding oxidative co-factors like cobalt-based co-catalysts[19] (e.g., Co_3O_4, a sustainable oxygen-evolution catalyst) are desirable to promote the fast interfacial transfer of the holes, and avoid surface-charge build up. This can in principle also favor the reductive reaction (hydrogen evolution) owing to the resultant fast charge separation and transformation at the interfaces.

In summary, the H_2 production performance of mpg-CN under visible light is significantly improved by growing thin layers of MoS_2 on mpg-CN. The 0.5 wt% MoS_2/mpg-CN performs better than 0.5 wt% Pt/mpg-CN under identical reaction conditions. The geometric similarity in the layered structures of MoS_2 and g-CN, together with the mesoporous structure of mpg-CN facilitates the planar growth of MoS_2 over the mpg-CN surface and the formation of the thin, planar MoS_2/mpg-CN interface; these characteristics are believed to promote the photoactivity of MoS_2/mpg-CN. We found that other layered transition metal dichalcogenides such as WS_2 are also efficient promoters for hydrogen production over g-CN (see the Supporting Information, Table S1). Herein we have presented not only an example of a catalyst made of abundant C, N, Mo and S elements for efficient H_2 photosynthesis, but also a conceptual advance to rationally design and fabricate a thin, effective interfacial 2D junctions between co-catalysts and semiconductors that have similar layered geometric structures.

Received: December 26, 2012
Published online: February 20, 2013

Keywords: co-catalysts · hydrogen · MoS_2 · organic–inorganic hybrid compounds · photocatalysis

[1] a) J. A. Turner, *Science* **2004**, *305*, 972; b) N. S. Lewis, D. G. Nocera, *Proc. Natl. Acad. Sci. USA* **2006**, *103*, 15729.
[2] a) A. Fujishima, K. Honda, *Nature* **1972**, *238*, 37; b) F. T. Wagner, G. A. Somorjai, *Nature* **1980**, *286*, 474; c) Z. G. Zou, J. H. Ye, K. Sayama, *Nature* **2001**, *414*, 625; d) H. Kato, K. Asakura, A. Kudo, *J. Am. Chem. Soc.* **2003**, *125*, 3082; e) K. Maeda, K. Teramura, D. L. Lu, T. Takata, N. Saito, Y. Inoue, K. Domen, *Nature* **2006**, *440*, 295; f) X. B. Chen, S. H. Shen, L. J. Guo, S. S. Mao, *Chem. Rev.* **2010**, *110*, 6503.
[3] a) M. G. Walter, E. L. Warren, J. R. McKone, S. W. Boettcher, Q. X. Mi, E. A. Santori, N. S. Lewis, *Chem. Rev.* **2010**, *110*, 6446; b) K. Maeda, *J. Photochem. Photobiol. C* **2011**, *12*, 237; c) Y. Tachibana, L. Vayssieres, J. R. Durrant, *Nat. Photonics* **2012**, *6*, 511.
[4] a) A. Heller, E. Aharon-Shalom, W. A. Bonner, B. Miller, *J. Am. Chem. Soc.* **1982**, *104*, 6942; b) Y. Shimodaira, A. Kudo, H. Kobayashi, *Chem. Lett.* **2007**, *36*, 170; c) J. Zhang, Q. Xu, Z. C. Feng, M. J. Li, C. Li, *Angew. Chem.* **2008**, *120*, 1790; *Angew. Chem. Int. Ed.* **2008**, *47*, 1766; d) X. Wang, L. Yin, G. Liu, L, Wang, R. Saito, G. Q. Lu, H. M. Cheng, *Energy Environ. Sci.* **2011**, *4*, 3976; e) H. W. Kang, S. N. Lim, D. Song, S. B. Park, *Int. J. Hydrogen Energy* **2012**, *16*, 11602.
[5] a) X. C. Wang, K. Maeda, A. Thomas, K. Takanabe, G. Xin, K. Domen, M. Antonietti, *Nat. Mater.* **2009**, *8*, 76; b) J. S. Zhang, X. F. Chen, K. Takanabe, K. Maeda, K. Domen, J. D. Epping, X. Z. Fu, M. Antonietti, X. C. Wang, *Angew. Chem.* **2010**, *122*, 451; *Angew. Chem. Int. Ed.* **2010**, *49*, 441.
[6] a) X. C. Wang, K. Maeda, X. F. Chen, K. Takabe, K. Domen, Y. D. Hou, X. Z. Fu, M. Antonietti, *J. Am. Chem. Soc.* **2009**, *131*, 1680; b) J. H. Sun, J. S. Zhang, M. W. Zhang, M. Antonietti,

X. Z. Fu, X. C. Wang, *Nat. Commun.* **2012**, *3*, 1139; c) J. S. Zhang, M. W. Zhang, R. Q. Sun, X. C. Wang, *Angew. Chem.* **2012**, *124*, 10292; *Angew. Chem. Int. Ed.* **2012**, *51*, 10145; d) Y. J. Cui, Z. X. Ding, X. Z. Fu, X. C. Wang, *Angew. Chem.* **2012**, *124*, 11984; *Angew. Chem. Int. Ed.* **2012**, *51*, 11814; e) Z. Z. Lin, X. C. Wang, *Angew. Chem.* **2013**, *125*, 1779; *Angew. Chem. Int. Ed.* **2013**, *52*, 1735.

[7] a) K. Maeda, X. C. Wang, Y. Nishihara, D. L. Lu, M. Antonietti, K. Domen, *J. Phys. Chem. C* **2009**, *113*, 4940; b) Y. Di, X. C. Wang, A. Thomas, M. Antonietti, *ChemCatChem* **2010**, *2*, 834.

[8] P. C. K. Vesborg, T. F. Jaramillo, *RSC Adv.* **2012**, *2*, 7933.

[9] a) D. Merki, X. L. Hu, *Energy Environ. Sci.* **2011**, *4*, 3878; b) A. B. Laursen, S. Kegnaes, S. Dahl, I. Chorkendorff, *Energy Environ. Sci.* **2012**, *5*, 5577.

[10] a) B. Hinnemann, P. G. Moses, J. Bonde, K. P. Jørgensen, J. H. Nielsen, S. Horch, I. Chorkendorff, J. K. Nørskov, *J. Am. Chem. Soc.* **2005**, *127*, 5308; b) T. F. Jaramillo, K. P. Jørgensen1, J. Bonde, J. H. Nielsen, S. Horch, I. Chorkendorff1, *Science* **2007**, *317*, 5834; c) J. Kibsgaard, Z. B. Chen, B. N. Reinecke, T. F. Jaramillo, *Nat. Mater.* **2012**, *11*, 963.

[11] Y. G. Li, H. L. Wang, L. M. Xie, Y. Y. Liang, G. S. Hong, H. J. Dai, *J. Am. Chem. Soc.* **2011**, *133*, 7296.

[12] a) T. F. Jaramillo, J. Bonde, J. D. Zhang, B. L. Ooi, K. Andersson, J. Ulstrup, I. Chorkendorff, *J. Phys. Chem. C* **2008**, *112*, 17492; b) Y. D. Hou, B. L. Abrams, P. C. K. Vesborg, M. E. Björketun, K. Herbst, L. Bech, A. M. Setti, C. D. Damsgaard, T. Pedersen, O. Hansen, J. Rossmeisl, S. Dahl, J. K. Nørskov, I. Chorkendorff, *Nat. Mater.* **2011**, *10*, 434; c) D. Merki, S. Fierro, H. Vrubel, X. L. Hu, *Chem. Sci.* **2011**, *2*, 1262.

[13] a) X. Zong, H. J. Yan, G. P. Wu, G. J. Ma, F. Y. Wen, L. Wang, C. Li, *J. Am. Chem. Soc.* **2008**, *130*, 7176; b) M. L. Tang, D. C. Grauer, B. Lassalle-kaiser, V. K. Yachandra, L. Amirav, J. R. Long, J. Yano, A. P. Alivisatos, *Angew. Chem.* **2011**, *123*, 10385; *Angew. Chem. Int. Ed.* **2011**, *50*, 10203; c) Q. J. Xiang, J. G. Yu, M. Jaroniec, *J. Am. Chem. Soc.* **2012**, *134*, 6575; d) B. Seger, A. B. Laursen, P. C. K. Vesborg, T. Pedersen, O. Hansen, S. Dahl, I. Chorkendorff, *Angew. Chem.* **2012**, *124*, 9262; *Angew. Chem. Int. Ed.* **2012**, *51*, 9128.

[14] a) T. R. Thurston, J. P. Wilcoxon, *J. Phys. Chem. B* **1999**, *103*, 11; b) K. F. Mak, C. Lee, J. Hone, J. Shan, T. F. Heinz, *Phys. Rev. Lett.* **2010**, *105*, 136805.

[15] a) R. R. Lunt, K. Sun, M. Kroger, J. B. Benziger, S. R. Forrest, R. Stephen, *Phys. Rev. B* **2011**, *83*, 064114; b) Y. J. Hong, T. Fukui, *ACS Nano* **2011**, *5*, 7575.

[16] J. S. Zhang, M. Grzelczak, Y. D. Hou, K. Maeda, K. Domen, X. Z. Fu, M. Antonietti, X. C. Wang, *Chem. Sci.* **2012**, *3*, 443.

[17] F. A. Frame, F. E. Osterloh, *J. Phys. Chem. C* **2010**, *114*, 10628.

[18] H. Tributsch, J. C. Bennett, *J. Electroanal. Chem.* **1977**, *81*, 97.

[19] a) A. Kay, I. Cesar, M. Gratzel, *J. Am. Chem. Soc.* **2006**, *128*, 15714; b) M. W. Kanan, D. G. Nocera, *Science* **2008**, *321*, 10721027; c) F. Jiao, F. Heinz, *Angew. Chem.* **2009**, *121*, 1873; *Angew. Chem. Int. Ed.* **2009**, *48*, 1841.

